

Published in final edited form as:

Expert Rev Anticancer Ther. 2014 December ; 14(12): 1411–1418. doi:10.1586/14737140.2014.978293.

Nanotube x-ray for cancer therapy: a compact microbeam radiation therapy system for brain tumor treatment

Lei Zhang^{*,1}, Hong Yuan^{2,3}, Christina Inscoe^{1,4}, Pavel Chtcheprov⁵, Michael Hadsell^{4,6}, Yueh Lee^{2,3,4,5,7}, Jianping Lu^{1,4}, Sha Chang^{4,5,7,8}, and Otto Zhou^{1,4,7}

¹Department of Applied Physical Sciences, University of North Carolina at Chapel Hill, Chapel Hill, NC 27599, USA

²Department of Radiology, University of North Carolina at Chapel Hill, Chapel Hill, NC 27599, USA

³Biomedical Research Imaging Center, University of North Carolina at Chapel Hill, Chapel Hill, NC 27599, USA

⁴Department of Physics and Astronomy, University of North Carolina at Chapel Hill, Chapel Hill, NC 27599, USA

⁵Department of Biomedical Engineering, University of North Carolina at Chapel Hill, Chapel Hill, NC 27599, USA

⁶Department of Radiation Oncology, Stanford University, Stanford, CA 94305, USA

⁷Lineberger Comprehensive Cancer Center, University of North Carolina at Chapel Hill, Chapel Hill, NC 27599, USA

⁸Department of Radiation Oncology, University of North Carolina at Chapel Hill, Chapel Hill, NC 27599, USA

Abstract

Microbeam radiation therapy (MRT) is a promising preclinical modality for cancer treatment, with remarkable preferential tumoricidal effects, that is, tumor eradication without damaging normal tissue functions. Significant lifespan extension has been demonstrated in brain tumor-bearing small animals treated with MRT. So far, MRT experiments can only be performed in a few synchrotron facilities around the world. Limited access to MRT facilities prevents this enormously promising radiotherapy technology from reaching the broader biomedical research community and hinders its potential clinical translation. We recently demonstrated, for the first time, the feasibility of generating microbeam radiation in a laboratory environment using a carbon nanotube x-ray source array and performed initial small animal studies with various brain tumor models. This new nanotechnology-enabled microbeam delivery method, although still in its infancy, has shown

© 2014 Informa UK Ltd

*Author for correspondence: leiz@email.unc.edu.
zhou@email.unc.edu

Financial & competing interests disclosure

No writing assistance was utilized in the production of this manuscript.

promise for achieving comparable therapeutic effects to synchrotron MRT and has offered a potential pathway for clinical translation.

Keywords

brain tumor; carbon nanotube; glioblastoma multiforme; image guidance; microbeam radiation therapy; temozolomide; U87MG glioma; x-ray; γ -H2AX

Brain cancer & radiation therapy

Brain cancer is one of the most aggressive terminal diseases despite significant effort and advancement in anticancer treatment. The median survival time for patients with glioblastoma multiforme, the most common and lethal form of brain tumor, is 15 months after diagnosis. There has been only minimal improvement over the past 50 years, even with aggressive multimodality treatments [1,2]. Almost all high-grade gliomas recur and there is virtually no long-term survival [3]. Currently, radiotherapy is used in conjunction with surgery and chemotherapy as the standard of care for brain cancer patients [4]. Modern radiation therapy (RT) techniques, such as intensity-modulated radiation therapy and stereotactic radiosurgery, strive to achieve dose conformality to the tumor target and minimal dose deposition to surrounding critical structures.

However, none of those focal RT techniques have been shown to be successful in achieving effective tumor control and in 90% of the cases tumors reoccur at the primary site [5,6]. One of the main reasons is that most malignant brain cancers are highly aggressive and infiltrative, that is, the tumor cells are highly proliferating and tend to invade into normal brain, leaving no well-defined margins between the tumor and surrounding normal tissue. This poses a great challenge in radiotherapy to minimize treatment toxicity to critical normal brain tissue and the CNS when a large planning target volume must be covered by high levels of radiation dose for complete tumor ablation. It is even more of an issue in treating radiation-sensitive pediatric brain cancer patients.

Microbeam radiation therapy

Microbeam radiation therapy (MRT) is a new treatment modality that is different from conventional external beam RT. Instead of depositing homogeneous radiation dose with a continuous broadbeam throughout the entire treatment region, MRT employs spatially fractionated, planar x-ray beams that range from 20 mm to a few hundred microns wide, separated by a distance several times of their beamwidth (FIGURE 1) [7–11]. These quasi-parallel orthovoltage microplanar beams deliver, within a single fraction, two orders of magnitude higher dose than that used in conventional RT. These microbeams create unique dose profiles of alternating peaks and valleys with high peak-to-valley-dose-ratios (PVDR) [12,13]. Synchrotron-based MRT studies using small animal tumor models have convincingly demonstrated that normal tissue can be well preserved and recover from radiation even at extremely high peak doses. This was achieved while simultaneously suppressing the growth of tumor tissue, or completely eradicating the tumor, in some cases [14–18]. The median survival time of MRT-treated small animals can be improved tenfold

compared to untreated controls [19]. The tumor tissue selectivity makes MRT an attractive modality for treatment of brain malignancies.

High peak dose for tumor eradication and low valley dose for normal tissue tolerance in submillimeter length scale are essential characteristics of the MRT dosimetry. This is, however, difficult to achieve with current commercial radiation sources. The clinically used mega-voltage linear accelerators create a large number of scattered, secondary charged particles in tissue, which, as a result, makes it difficult to retain a sharp beam profile (small penumbras) and high PVDR. Conventional orthovoltage x-ray tubes generate broad and divergent radiation with flux limited by anode heat management. To obtain the desired microbeam pattern with sufficiently high PVDR, a collimator with a narrow opening and a large aspect ratio must be applied to the intrinsically divergent beam, which blocks an overwhelming majority of the x-ray photon flux and results in a much reduced microbeam dose rate. The output power of conventional microfocus x-ray tubes with submillimeter focal spot sizes is significantly lower than what is needed for MRT [20–22].

The ability of MRT to outperform conventional broadbeam RT has been demonstrated by several synchrotron-based studies. Dilmanian *et al.* irradiated a group of 9L gliosarcoma-bearing rats with microbeams of various pitches and dose levels and compared them with the broadbeam-treated group [15,23]. The median survival time of all the MRT-treated groups was significantly longer than the broadbeam RT group. In another study with EMT-6 carcinoma-bearing mice, an improved therapeutic index was shown in the coplanar microbeam irradiated groups compared to the broadbeam-treated group [7].

Nanotechnology enables a compact microbeam delivery system

We developed a spatially distributed field emission x-ray source array technology using carbon nanotubes (CNT) [24] [25–27]. In contrast to the current thermionic x-ray sources, it uses an electric field to extract electrons from one or multiple CNT cathodes at room temperature, which are focused and accelerated to bombard an anode to generate x-ray radiation. The field emission technology opens up new possibilities in x-ray source design that are not easily accessible with the thermionic sources, including arrays with different source configurations and electronically programmable radiation. The medical applications of this technology have been demonstrated in high-resolution dynamic micro-CT [28]; stationary digital breast tomosynthesis [29,30], which is currently in clinical trial [31] and tomosynthesis guidance for radiotherapy [32].

With the distributed source array design, the electron beam can be spread from a single focal spot into one or multiple long and narrow focal tracks to increase the microbeam dose rate. The concept is illustrated in [FIGURE 2](#) in a ring-shaped configuration. Each x-ray source segment delivers a microbeam array to the tumor target, directed from different angles [27]. This is in essence equivalent to having a large number of high-power x-ray tubes irradiating an object simultaneously without the constraint of space, cost, power consumption and alignment difficulties. In addition to increased microbeam dose rate, the ring-shaped configuration is advantageous for human MRT where a high target dose and high beam mean energy is required. Such design can effectively reduce the valley dose at the entrance

and the toxicity to skin and subcutaneous tissue by distributing the total entrance dose over a larger skin area compared to the fixed, unidirectional configuration of synchrotron sources.

The x-ray radiation from a CNT source array is electronically controlled, and each source can be switched on and off individually and near-instantaneously. Such features ensure reliable radiation beam delivery and meet the clinical requirement for RT systems in terms of safety and reliability. The programmable sources allow physiologically gated radiation delivery, where radiation exposure is synchronized with the respiratory and cardiac signals, to minimize motion-induced microbeam blur during treatment [33,34].

A compact image-guided MRT prototype for small animal models

The first proof-of-principle device, as shown in FIGURE 3, employs a single linear CNT source array which projects a long and narrow focal track (162 × 14 mm) on a stationary tungsten anode [35]. A motorized microbeam collimation and alignment assembly aligns a 175 μm slit with the anode focal line and collimates the primary beam into a microbeam of adjustable width. The first prototype operates at 160 kVp anode voltage and 30 mA tube current, generating a 280 μm wide microbeam at the sample entrance plane (124 mm downstream from the focal track). The average microbeam dose rate is 1.2 Gy/min at the sample entrance plane [36]. Parallel microbeams are delivered by translating the sample perpendicularly to the beam plane in a step-and-shoot manner. An example of the microbeam pattern recorded by a Gafchromic EBT2 film (Ashland Advanced Materials, KY, USA) is shown in FIGURE 4. Three microbeams (280 μm wide) were delivered at 900 μm center-to-center distance yielding a PVDR of 16 [36,37]. This is well within the typical PVDR range that has been shown sufficient for retaining the normal tissue sparing effect in synchrotron MRT experiments [11,15]. More specifications of the first CNT-based MRT prototype is listed in TABLE 1.

Target identification and localization are critical for treatment planning and accurate dose delivery. This has not been fully addressed in previous synchrotron MRT experiments; no comprehensive image-guidance protocol for tumor visualization and targeting has been reported. A few recent studies have investigated the use of planar x-ray radiography [38,39] or propagation-based phase contrast portal imaging [40] as guidance for MRT, either for the tumor injection point or specific skull bony-landmark-based verifications. In our prototype, a high-resolution micro-CT scanner was integrated with the microbeam irradiator to facilitate target identification and accurate microbeam delivery. This micro-CT scanner contains a micro-focused CNT x-ray source and provides an image resolution of up to 70 μm [28]. The CT rotation isocenter is aligned with the microbeam treatment platform, and a connecting high-precision translation stage transports the sample to the microbeam treatment site after imaging. Generally, CT images are not ideal for brain tumor visualization due to beam hardening through the skull and the resultant low soft tissue contrast. A considerable dose of contrast agent is often required, which causes nephrotoxicity and complicates the treatment outcome. As a result, MRI is used for tumor visualization, and on-board x-ray imaging is used for skull structures and landmark localization. Registered images from the two modalities are used to identify the tumor, determine the microbeam treatment coordinates and plan treatment accordingly (FIGURE

5). A detailed protocol with 2D imaging and registration was previously reported [36]. Briefly, animals undergo MRI scans (9.4T MR scanner, Bruker BioSpin Corp., MA, USA) the day before MRT to delineate the tumor and find its location. x-ray imaging is performed prior to treatment to capture the bone structures and landmarks on the mouse bed. Animals are anesthetized and immobilized the same way on a customized mouse bed for both MRI and x-ray imaging. The MR images and x-ray radiographs are registered using a 2D rigid-body method to present the tumor location relative to the skull and landmarks. With the landmarks precalibrated as a reference to the microbeam location, the registered images provide the tumor coordinates in the microbeam treatment space, and enable accurate delivery of microbeams to the tumor target. Using brain tumor-bearing mice models, a microbeam targeting accuracy of 450 μm has been accomplished (FIGURE 6). This fast procedure allows for imaging and irradiating two animals simultaneously to improve the experimental throughput.

Preliminary animal studies with brain tumor-bearing mice

Small animal studies have been carried out including tumor growth control and survival studies with U87MG human glioma-bearing mice and radiobiological studies with medulloblastoma-bearing mouse pups. A variety of characterization techniques, including MRI and immunohistological bio-markers such as $\gamma\text{-H2AX}$, cleaved caspase-3, Ki67 and F4/80, were used to facilitate the interpretation of MRT radiobiology at the cellular level. In a study with U87 human glioma-bearing mice, arrays of single or multiple microbeams of up to 138 Gy/beam were delivered to the 2-mm (average diameter) brain tumors, with a tumor targeting accuracy of around 450 μm [36]. As shown in FIGURE 6, microbeam radiation-induced DNA double-strand breaks were clearly characterized histologically on $\gamma\text{-H2AX}$ -stained brain sections collected after animal euthanization. Pink stripes of $\gamma\text{-H2AX}$ -positive cells corresponded to the tracks of microbeam peaks across the brain tumors. The beamwidth on the stained tissue, measured by the mean full-width-half-maximum, was 350 μm . This was broader than the 280 mm beamwidth measured by Gafchromic EBT2 film at the mouse skin entrance, but slightly narrower than the exit beamwidth (380 μm). Beam center-to-center distance from the histology was 800 μm . Measurements from the histology matched well with the planned beam pitch and film results, when considering tissue distortion and the 20% anisotropic shrinkage during tissue processing [41]. In another study using the same animal models, $\gamma\text{-H2AX}$ expression was measured at 1, 4, 24 and 48 h after MRT and also at 7 days. Strong $\gamma\text{-H2AX}$ signal was observed at the early hours, and the expression reduced over time in both tumor and normal tissue. After 7 days, $\gamma\text{-H2AX}$ expression was still detected, although very weak. Quantitatively, higher level of $\gamma\text{-H2AX}$ expression was observed in the tumor region compared to that in normal tissue. The expression in tumor after 48 h was well dispersed with no clear delineation between peak and valley regions, whereas in normal tissue weak $\gamma\text{-H2AX}$ signals were only detected on the beam tracks.

In another study with U87 tumor mice, a significant decrease in the tumor growth rate was seen in the mice treated with microbeams compared to the nontreated sham control (FIGURE 7) [42]. Twenty young-adult athymic nude mice inoculated with U87MG human glioma tumor cells were grouped to receive different treatments. They were unidirectional two microbeams radiation with 48 Gy, 66 Gy, 72 Gy or 100 Gy peak entrance doses; two

orthogonally cross-fired arrays of four microbeams (crossbeam) with 50 Gy peak entrance dose and 10 Gy whole-brain broadbeam RT using a 6 MV clinical LINAC (Siemens Corp., Germany). The microbeams used in all MRT groups were approximately 300 μm wide and separated by 900 μm center-to-center distance. T2-weighted MRI volumetric results (FIGURE 7) pre- and post-treatment indicated that higher peak entrance doses produced more prominent tumor growth suppression. Animals treated with unidirectional high-dose MRT showed similar tumor growth delay compared to the conventional RT-treated group. Particularly, a better tumor local control was achieved in the group treated with crossbeam high-dose MRT (FIGURE 8).

Cardiac and respiration-induced brain motion in humans can range from a few hundred microns to 1 mm [43,44], which is similar to or even wider than the microbeams. To avoid beam blurring and/or false targeting caused by motion, it is necessary to either complete the treatment within a time window much shorter than the motion cycle or synchronize radiation exposure with the physiological motion. The former approach is used at the synchrotron MRT facilities where the dose rate can exceed 10^3 Gy/s. Physiological gating eliminates the need for this extraordinarily high dose rate that causes safety concerns and cannot be achieved by non-synchrotron radiation sources. The feasibility of physiologically gated micro-beam irradiation was recently demonstrated *in vivo*, for the first time, using our CNT-based MRT system [33,34]. The respiratory signals of an anesthetized mouse were recorded with a sensor, which triggered the microbeam radiation exposure during a specific phase of the respiratory cycle. Histological results showed that gated irradiation can effectively reduce motion-induced beam broadening and improve the overall PVDR [34].

Expert commentary & five-year view

The research on MRT has been limited to a few synchrotron facilities around the world since the beginning in 1960s, due to the lack of appropriate non-synchrotron delivery technologies. The novel CNT x-ray source array makes it possible to develop, for the first time, compact laboratory-scale MRT systems for cancer research and provides a potential pathway for clinical translation. Compared to the current synchrotron-based MRT facilities, CNT-based MRT also has several intrinsic advantages, including orders of magnitude lower in dimensions and cost. The physiologically gated irradiation minimizes motion-induced microbeam blur and eliminates the need for the ultra-high dose rate, which is a concern for patient safety. The surrounding source design (as shown in FIGURE 2) with conformal collimation can provide a more desirable dose profile than the unidirectional beam, resulting in a higher energy deposited on the tumor than on the skin [45]. Different micro-beam treatment patterns such as interlaced microbeams can be generated in a single fraction without patient translation or rotation.

The results, so far, show that the essential dosimetry characteristics that are considered necessary for the unique preferential tumoricidal effects of MRT – including beam energy, beam width and PVDR – can be generated by the CNT-based MRT system. Preliminary studies using small animal models have shown promising therapeutic effects in terms of tumor local control and survival rate extension. The research is still in its infancy and the technology needs further development. The first-generation prototype produces a single

microbeam at a low average microbeam dose rate due to the limit of the anode heat dissipation capability. The low dose rate limits the experimental output and poses challenges in animal anesthetization and immobilization. The mean beam energy of the prototype is approximately 60 keV, lower than the value used in the synchrotron MRT which is typically around 100 keV. Additionally, the beamwidth from the first prototype is 280 μm , which is slightly wider than the typical 25–75 μm beamwidth used in early synchrotron studies. However, there have been many reports that demonstrated similar therapeutic effects with larger size microbeams (up to 700 μm wide) [8,9,46–48]. Our beamwidth is well within the size range that has been shown to retain the MRT therapeutic effects.

A second-generation system has been designed and is being assembled and tested. The new CNT source array has a significantly increased anode heat capacity. It will be able to generate multiple parallel microbeams with an anticipated 20-times increase in the dose rate and a higher x-ray mean energy compared to the first-generation system. The higher flux allows delivery of a total MRT dose comparable to that used in synchrotron MRT studies, within an acceptable time window.

To translate MRT from a highly promising radiotherapy technology for experimental small animal studies to patient treatment, many challenges and unanswered questions need to be first addressed. In the next 5 years, we expect that the potential of MRT for large animal and human treatment will be evaluated at synchrotron facilities, and we will continue the development of laboratory-scale MRT systems to facilitate the research and translation of this promising technology. After many years of comprehensive research using small animal models, the group at the European Synchrotron Radiation Facility has initiated a study using brain tumor-bearing larger animals including dogs and cats [49,50]. This is a major step toward patient treatment. It remains to be seen whether the MRT preferential therapeutic effects are maintained in larger animals. Optimization of the corresponding dosimetric parameters to adapt to larger treatment targets will be also needed.

Although MRT as an experimental RT modality has been studied for several decades, today it remains an unfamiliar technique to most medical physicists and radiation oncologists, and is pursued only by a few research groups with access to the limited number of synchrotron facilities around the world. We hope the availability of this compact and economically viable MRT technology will encourage more researchers to investigate this promising radiotherapy technique and expedite its potential clinical translation.

Acknowledgments

This work is supported by the National Cancer Institute (NCI)-funded Carolina Center for Cancer Nanotechnology Excellence (U54-CA151652) and the NCI Grand Opportunity grant (RC2-CA 148487). The CNT x-ray source array was manufactured by XinRay Systems. The U87 glioma cells were kindly provided by Dr. Ryan Miller's lab at University of North Carolina at Chapel Hill Department of Pathology. The authors would also like to thank J Tepper at UNC Radiation Oncology for helpful discussions.

References

Papers of special note have been highlighted as:

- of interest

•• of considerable interest

1. Huse JT, Holland EC. Targeting brain cancer: advances in the molecular pathology of malignant glioma and medulloblastoma. *Nat Rev Cancer*. 2010; 10(5):319–31. [PubMed: 20414201]
2. Zhang J, Stevens MF, Bradshaw TD. Temozolomide: mechanisms of action, repair and resistance. *Curr Mol Pharmacol*. 2012; 5(1):102–14. [PubMed: 22122467]
3. Behin A, Hoang-Xuan K, Carpentier AF, Delattre JY. Primary brain tumours in adults. *Lancet*. 2003; 361(9354):323–31. [PubMed: 12559880]
4. Sengupta S, Marrinan J, Frishman C, Sampath P. Impact of temozolomide on immune response during malignant glioma chemotherapy. *Clin Dev Immunol*. 2012; 2012:831090. [PubMed: 23133490]
5. Jov evska I, Ko evar N, Komel R. Glioma and glioblastoma - how much do we (not) know? *Mol Clin Oncol*. 2013; 1(6):935–41. [PubMed: 24649273]
6. Matinfar M, Ford E, Iordachita I, et al. Image-guided small animal radiation research platform: calibration of treatment beam alignment. *Phys Med Biol*. 2009; 54(4):891–905. [PubMed: 19141881]
7. Dilmanian FA, Morris GM, Zhong N, et al. Murine EMT-6 carcinoma: high therapeutic efficacy of microbeam radiation therapy. *Radiat Res*. 2003; 159(5):632–41. [PubMed: 12710874]
8. Dilmanian FA, Qu Y, Liu S, et al. X-ray microbeams: Tumor therapy and central nervous system research. *Nucl Instrum Methods Phys Res A*. 2005; 548(1-2):30–7. [PubMed: 17369874]
9. Dilmanian FA, Zhong Z, Bacarian T, et al. Interlaced x-ray microplanar beams: a radiosurgery approach with clinical potential. *Proc Natl Acad Sci USA*. 2006; 103(25):9709–14. [PubMed: 16760251]
10. Serduc R, Bouchet A, Bräuer-Krisch E, et al. Synchrotron microbeam radiation therapy for rat brain tumor palliation—influence of the microbeam width at constant valley dose. *Phys Med Biol*. 2009; 54(21):6711. [PubMed: 19841517]
11. Ansel DJ, Bravin A, Romanelli P. Microbeam radiosurgery using synchrotron-generated submillimetric beams: a new tool for the treatment of brain disorders. *Neurosurg Rev*. 2010; 34(2): 133–42. [PubMed: 21088863]
12. Slatkin DN, Spanne P, Dilmanian FA, Sandborg M. Microbeam radiation therapy. *Med Phys*. 1992; 19(6):1395–400. [PubMed: 1461201]
13. Laissue, JA.; Lyubimova, N.; Wagner, H-P., et al. Microbeam radiation therapy.. Presented at SPIE; Denver, CO USA. 1999;
14. Laissue JA, Geiser G, Spanne PO, et al. Neuropathology of ablation of rat gliosarcomas and contiguous brain tissues using a microplanar beam of synchrotron-wiggler-generated X rays. *Int J Cancer*. 1998; 78(5):654–60. [PubMed: 9808538]
15. Dilmanian FA, Button TM, Le Duc G, et al. Response of rat intracranial 9L gliosarcoma to microbeam radiation therapy. *Neuro-oncol*. 2002; 4(1):26–38. [PubMed: 11772430]
16. Zhong N, Morris GM, Bacarian T, et al. Response of rat skin to high-dose unidirectional x-ray microbeams: a histological study. *Radiat Res*. 2003; 160(2):133–42. [PubMed: 12859223]
17. Regnard P, Le Duc G, Brauer-Krisch E, et al. Irradiation of intracerebral 9L gliosarcoma by a single array of microplanar x-ray beams from a synchrotron: balance between curing and sparing. *Phys Med Biol*. 2008; 53(4):861–78. [PubMed: 18263945]
18. Crosbie JC, Anderson RL, Rothkamm K, et al. Tumor cell response to synchrotron microbeam radiation therapy differs markedly from cells in normal tissues. *Int J Radiat Oncol Biol Phys*. 2010; 77(3):886–94. [PubMed: 20510199]
- 19•. Serduc R, Brauer-Krisch E, Bouchet A, et al. First trial of spatial and temporal fractionations of the delivered dose using synchrotron microbeam radiation therapy. *J Synchrotron Radiat*. 2009; 16(Pt 4):587–90. [PubMed: 19535875] [Reported the method of delivering arrays of microbeams from multiple ports and cross-firing at the mouse brain tumor, and achieved the longest mean survival tumor so far using microbeam radiation therapy (MRT) for the highly aggressive 9L tumor model.]
20. Grider DE, Wright A, Ausburn PK. Electron-Beam Melting in Microfocus X-Ray Tubes. *J Phys D- Appl Phys*. 1986; 19(12):2281–92.

21. Flynn MJ, Hames SM, Reimann DA, Wilderman SJ. Microfocus X-Ray Sources for 3d Microtomography. *Nucl Instrum Methods Phys Res A -Accelerators Spectrometers Detectors and Associated Equipment*. 1994; 353(1-3):312–15.
22. Shan, J.; Zhou, OT.; Lu, JP. Anode thermal analysis of high power micro-focus CNT X-ray tubes for in-vivo small animal imaging.. Presented at Proc Spie; San Diego, California, USA. 2012;
23. Joel DD, Fairchild RG, Laissie JA, et al. Boron neutron capture therapy of intracerebral rat gliosarcomas. *Proc Natl Acad Sci USA*. 1990; 87(24):9808–12. [PubMed: 2263630]
24. Zhou, O.; Calderon-Colon, X. Chapter 26. Carbon Nanotube-Based Field Emission X-Ray Technology.. In: SaitM, Y., editor. Carbon Nanotube and Related Field Emitters. Wiley-VCH; Weinheim: 2010. p. 417-37.
25. Zhou, OZ.; Lu, J. X-ray generating mechanism using electron field emission cathode.. 2003. US6,553,096 B1
26. Zhou, O.; Lu, J.; Qiu, Q. Large-area individually addressable multi-beam x-ray system and method of forming same.. 2005. US6876724 B2
27. Zhou, OZ.; Chang, SX. Compact microbeam radiation therapy systems and methods for cancer treatment and research.. 2010. US8,600,003
28. Cao G, Lee YZ, Peng R, et al. A dynamic micro-CT scanner based on a carbon nanotube field emission x-ray source. *Phys Med Biol*. 2009; 54:2323–40. [PubMed: 19321922]
29. Qian X, Rajaram R, Calderon-Colon X, et al. Design and characterization of a spatially distributed multi-beam field emission x-ray source for stationary digital breast tomosynthesis. *Med Phys*. 2009; 36(10):4389. [PubMed: 19928069]
30. Qian X, Tucker A, Gidcumb E, et al. High resolution stationary digital breast tomosynthesis using distributed carbon nanotube x-ray source array. *Med Phys*. 2012; 39(4):2090–9. [PubMed: 22482630]
31. Comparison of Stationary Breast Tomosynthesis and 2-D Digital Mammography in Patients With Known Breast Lesions. Available from: <https://clinicaltrials.gov/ct2/show/NCT01773850> [The first CNT X-ray technology-based medical imaging system undergoing clinical trial.]
32. Maltz JS, Sprenger F, Fuerst J, et al. Fixed gantry tomosynthesis system for radiation therapy image guidance based on a multiple source x-ray tube with carbon nanotube cathodes. *Med Phys*. 2009; 36(5):1624–36. [PubMed: 19544779]
33. Chtcheprov, P.; Hadsell, M.; Burk, L., et al. Physiologically gated micro-beam radiation therapy using electronically controlled field emission x-ray source array.. Presented at Proc Spie; Lake Buena Vista (Orlando Area), Florida USA. 2013.
34. Chtcheprov P, Burk L, Yuan H, et al. Physiologically gated microbeam radiation using a field emission x-ray source array. *Med Phys*. 2014; 41(8):081705. [PubMed: 25086515]
35. Hadsell M, Zhang J, Laganis P, et al. A first generation compact microbeam radiation therapy system based on carbon nanotube X-ray technology. *Appl Phys Lett*. 2013; 103(18):183505. [PubMed: 24273330] [Described some technical specifications of the first prototype carbon nanotube (CNT)-based compact MRT system.]
36. Zhang L, Yuan H, Burk LM, et al. Image-guided microbeam irradiation to brain tumour bearing mice using a carbon nanotube x-ray source array. *Phys Med Biol*. 2014; 59(5):1283–303. [PubMed: 24556798] [Reported the MRI/X-ray combined image-guidance protocol and targeting verification using U87MG glioma-bearing mice and γ -H2AX immunohistological staining.]
37. Hadsell, M. PhD Thesis. University of North Carolina at Chapel Hill; 2013. The development and characterization of a first generation carbon nanotube x-ray based microbeam radiation therapy system..
38. Serduc R, Berruyer G, Brochard T, et al. In vivo pink-beam imaging and fast alignment procedure for rat brain lesion microbeam radiation therapy. *J Synchrotron Radiat*. 2010; 17(3):325–31. [PubMed: 20400830]
39. Romanelli P, Fardone E, Battaglia G, et al. Synchrotron-generated microbeam sensorimotor cortex transections induce seizure control without disruption of neurological functions. *PLoS One*. 2013; 8(1):e53549. [PubMed: 23341950]
40. Umetani, K.; Kondoh, T. Phase contrast portal imaging for image-guided microbeam radiation therapy.. Presented at Proc Spie; 2014.

41. Winsor, L. Tissue processing.. In: Woods, AE.; Ellis, RC., editors. *Laboratory Histopathology*. Churchill Livingstone; New York: 1994. p. 4.2-1-4.2-39.
42. Yuan H, Zhang L, Frank JE, et al. Treating brain tumor with microbeam radiation generated by a compact carbon-nanotube-based irradiator: initial radiation efficacy study. *Radiat Res*. 2014 (Submitted).
43. Zhong XD, Meyer CH, Schlesinger DJ, et al. Tracking brain motion during the cardiac cycle using spiral cine-DENSE MRI. *Med Phys*. 2009; 36(8):3413–19. [PubMed: 19746774]
44. Wu D, Hatfield J, Modi J, Mathew G. When does brain motion interfere with the accuracy of stereotactic radiosurgery? Investigation of brain motion in the presence of stereotactic Frame. Presented at Proc Intl Soc Mag Reson Med. 2010
45. Schreiber EC, Chang SX. Monte Carlo simulation of a compact microbeam radiotherapy system based on carbon nanotube field emission technology. *Med Phys*. 2012; 39(8):4669–78. [PubMed: 22894391]
46. Prezado, Y.; Renier, M.; Bravin, A. A new synchrotron radiotherapy technique with future clinical potential: minibeam radiation therapy.. Presented at: IFMBE; Munich, Germany. 2009;
47. Prezado Y, Sarun S, Gil S, et al. Increase of lifespan for glioma-bearing rats by using minibeam radiation therapy. *J Synchrotron Radiat*. 2012; 19(Pt 1):60–5. [PubMed: 22186645]
48. Gil S, Sarun S, Biete A, et al. Survival analysis of F98 glioma rat cells following minibeam or broad-beam synchrotron radiation therapy. *Radiat Oncol*. 2011; 6:37. [PubMed: 21489271]
49. Requardt H, Bravin A, Prezado Y, et al. The clinical trials program at the ESRF biomedical beamline ID17: status and Remaining Steps. *AIP Conf Proc*. 2010; 1234(1):161–4.
50. Bartzsch S, Lerch M, Petasecca M, et al. Influence of polarization and a source model for dose calculation in MRT. *Med Phys*. 2014; 41(4):041703. [PubMed: 24694123]

Key issues

- Brain tumors, especially glioblastoma multiforme, are among the most deadly cancers. So far, there has been no effective treatment to significantly extend the patients' mean survival. Clinically used RT modalities often cause intolerable normal tissue toxicity to the circumjacent critical brain structures and the CNS.
- Microbeam radiation therapy (MRT) in small animal tumor models has shown strong tumor killing and normal tissue sparing effects.
- Until now, MRT research can only be carried out at a few remote synchrotron facilities and the therapeutic mechanism behind is still unclear. Widely accessible microbeam irradiators that can be readily installed in laboratories and medical centers are needed.
- Carbon nanotube (CNT) x-ray technology overcomes some of the limitations of conventional orthovoltage tubes and is the core of our technique for developing a compact MRT system for preclinical and, ultimately, clinical use.
- Utilizing the CNT source array, a prototype CNT-based microbeam irradiator has been developed and calibrated for preclinical studies.
- An MRI/x-ray combined image guidance protocol has been demonstrated to achieve a targeting accuracy of 450 μ m in brain tumor mouse models.
- Preliminary studies in U87MG human glioma-bearing mice using the CNT MRT prototype have shown significant tumor growth suppression in MRT-treated groups compared to nontreated controls.
- Gated MRT is feasible using our proof-of-concept MRT prototype. It has been shown to be effective in reducing motion-induced microbeam blurring.

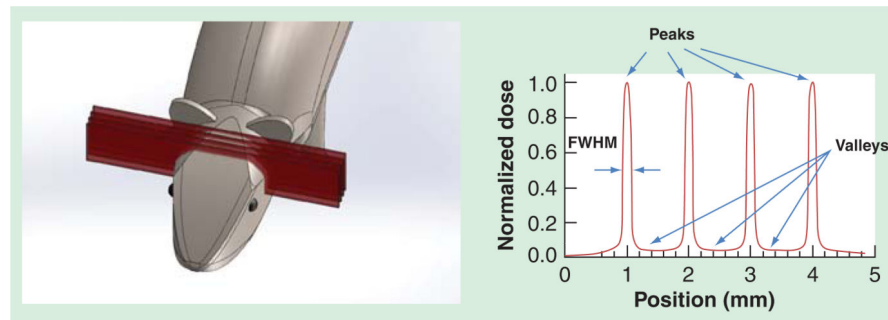


Figure 1. Left: SolidWorks drawing of an array of microbeams irradiating the mouse brain. Right: Illustration of idealized microbeam radiation therapy dose distribution with alternating peaks and valleys and a high peak-to-valley-dose-ratio. The beam width measured in FWHM is usually around 25 μm or up to 700 μm . FWHM: Full-width-half-maximum.

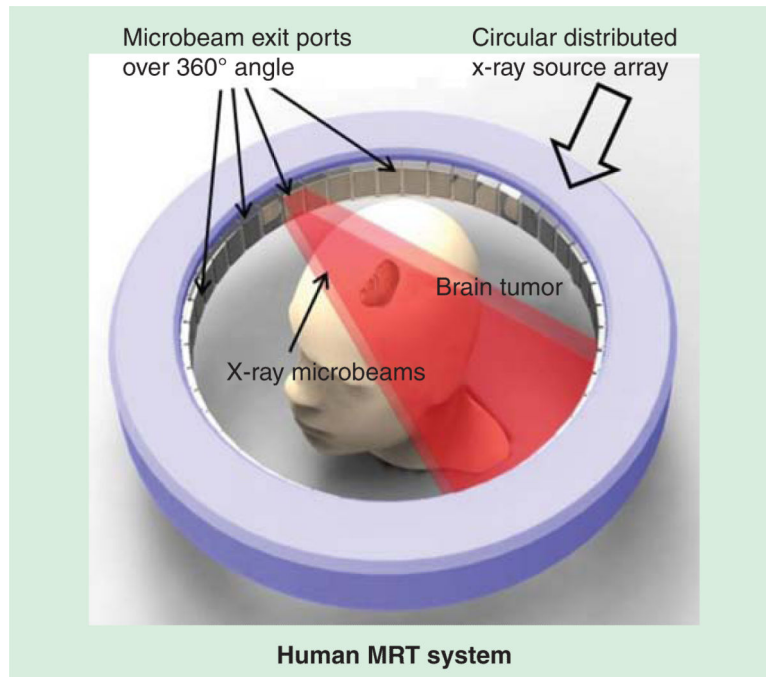


Figure 2. A conceptual SolidWorks drawing of a ring-structure human carbon nanotube-microbeam radiation therapy system, where microbeams come from multiple ports and are directed toward the treatment target simultaneously.

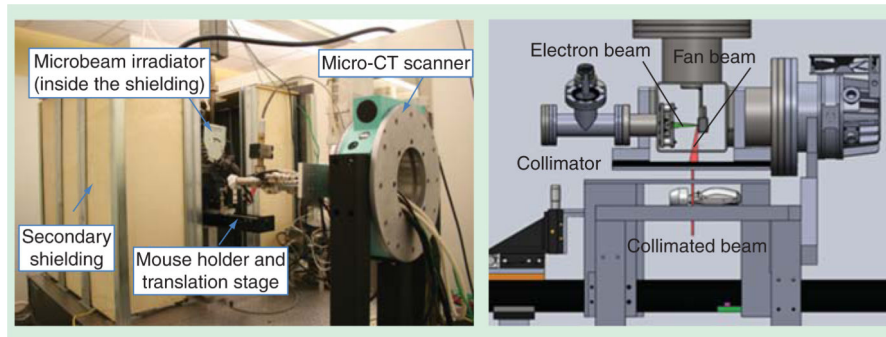


Figure 3.

Left: A photo of the first prototype image-guided microbeam irradiation system in our lab. Right: A SolidWorks drawing illustrating our first prototype carbon nanotube microbeam radiation therapy system which consists of a single array of carbon nanotube x-ray source. Electron beam generation, x-ray microbeam collimation and the microbeam irradiating a mouse head have been indicated. Reproduced with permission from [36].

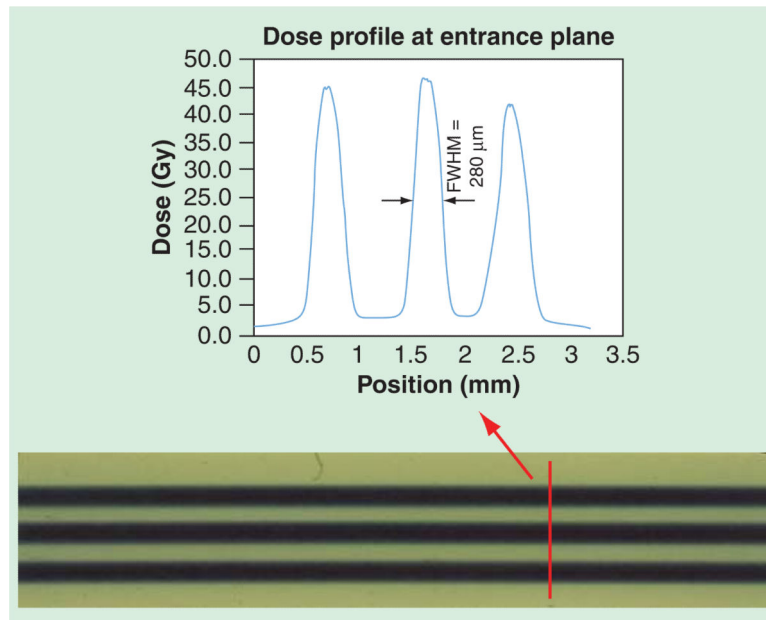


Figure 4. Dose profile at entrance plane of U87 tumor mice microbeam radiation therapy, recorded by Gafchromic EBT2 film and analyzed using FilmQAPro program (multi-channel dosimetry) (Ashland Advanced Materials, KY, USA). The peak-to-valley-dose-ratio was measured to be 16 with 280- μm wide microbeams separated at 900 μm center-to-center distance. FWHM: Full-width-half-maximum.

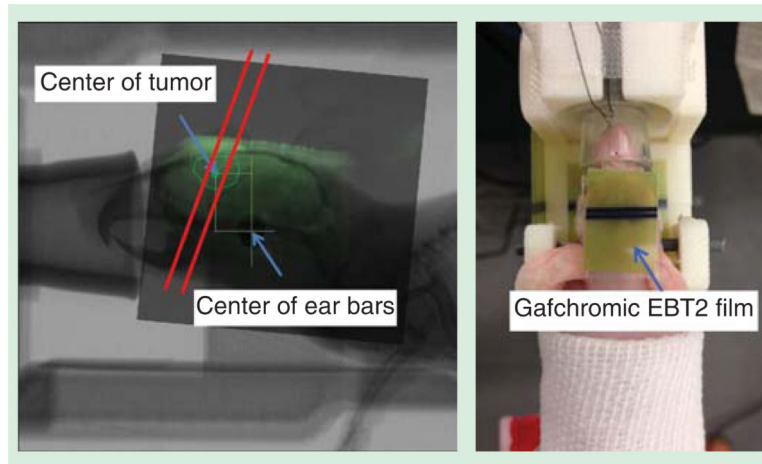


Figure 5. Left: A 2D registered image of MR image and X-ray radiograph, with three microbeams planned to irradiate across the tumor area; Right: a picture of U87 glioma-bearing mouse fully stabilized on the homemade holder with ear bar and teeth fixation. Gafchromic EBT2 film was used at the microbeam entrance and exit plane for dosimetry confirmation purposes.

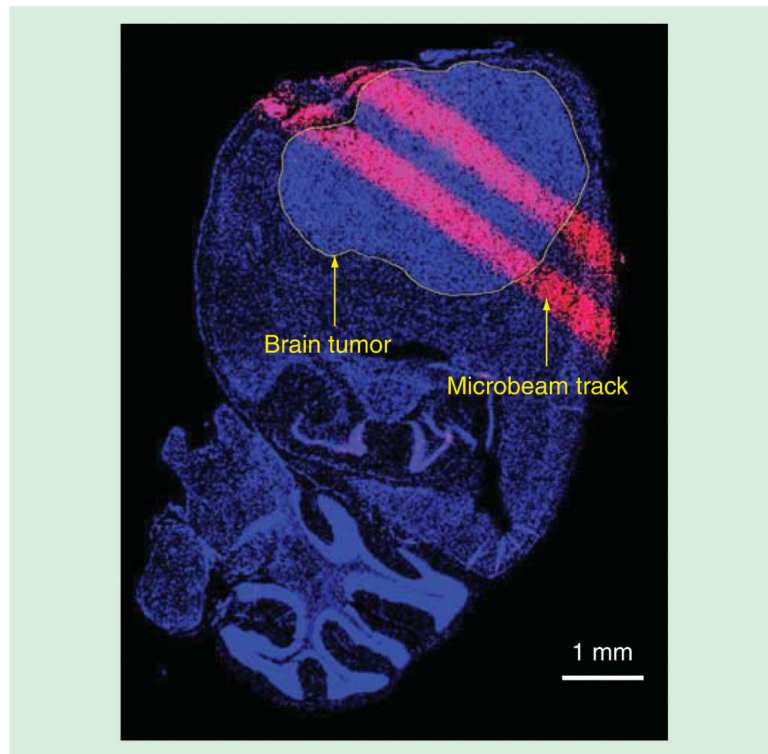


Figure 6. γ -H2AX staining of the brain tissue collected from the tumor mouse treated with two-beam microbeam radiation therapy. The animal was sacrificed and the brain was collected and fixed 4 h after radiation finished. Reproduced with permission from [33].

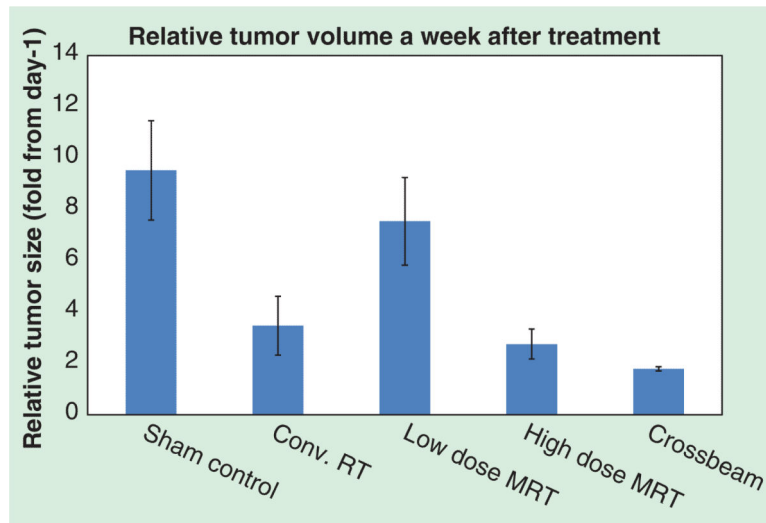


Figure 7. MRI volumetric data showing the relative tumor volume growth of U87 glioma-bearing mice a week after receiving different treatments. Notice the trend of decreased growth rate with increasing MRT peak entrance dose. Notice the animal treated with crossbeam MRT showed minimum relative tumor growth. Conv. RT: Conventional radiation therapy; MRT: Microbeam radiation therapy.

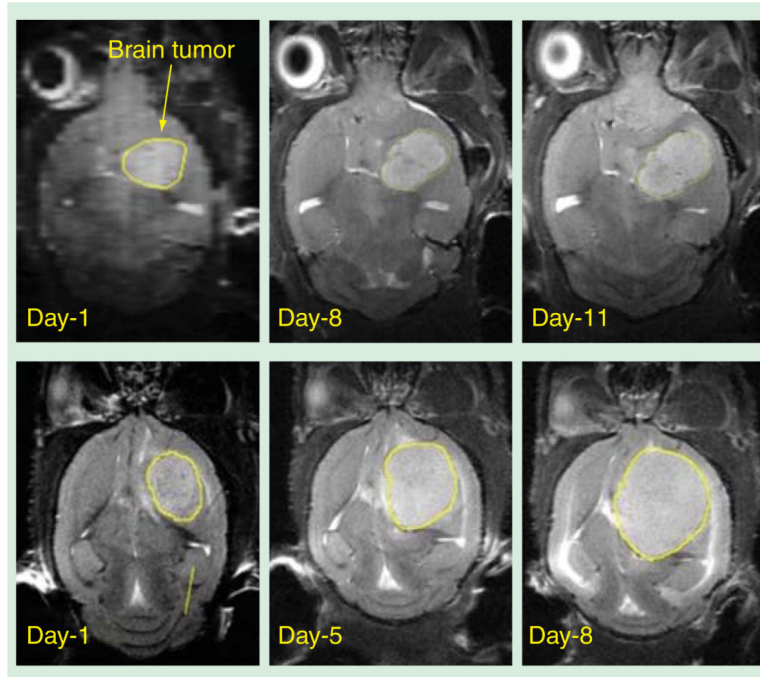


Figure 8. Volumetric data from T2-weighted MRI of two U87 glioma-bearing mice treated with crossbeam microbeam radiation therapy (top) and conventional whole brain broadband radiation therapy (bottom).

Table 1

Specifications of the first prototype CNT-based MRT system.

Parameters	CNT-based MRT
Number of CNT source arrays	1
Anode voltage	160 kV
Tube current	30 mA
Focal track width	131 μm
Average entrance dose rate [†]	1.2 Gy/min
Entrance microbeam width [†]	280 μm
Entrance PVDR [†]	17 (beam separation 900 μm)
On-board imager	Micro-CT
Physiological gating capability	Yes

CNT: Carbon nanotube; MRT: Microbeam radiation therapy; PVDR; Peak-to-valley-dose-ratio.

[†] Measured at 124 mm from the focal track on the anode.